TPX2 phosphorylation maintains metaphase spindle length by regulating microtubule flux

Jingyan Fu,[1,2]* Minglei Bian,[1,2]* Guangwei Xin,[1,2] Zhaoxuan Deng,[1,2] Jia Luo,[1,2] Xiao Guo,[1,2] Hao Chen,[1,2] Yao Wang,[1,2] Qing Jiang,[1,2] and Chuanmao Zhang[1,2]

[1]The Ministry of Education Key Laboratory of Cell Proliferation and Differentiation and [2]The State Key Laboratory of Bio-membrane and Membrane Biotechnology, College of Life Sciences, Peking University, Beijing 100871, China

A steady-state metaphase spindle maintains constant length, although the microtubules undergo intensive dynamics. Tubulin dimers are incorporated at plus ends of spindle microtubules while they are removed from the minus ends, resulting in poleward movement. Such microtubule flux is regulated by the microtubule rescue factors CLASPs at kinetochores and depolymerizing protein Kif2a at the poles, along with other regulators of microtubule dynamics. How microtubule polymerization and depolymerization are coordinated remains unclear. Here we show that TPX2, a microtubule-bundling protein and activator of Aurora A, plays an important role. TPX2 was phosphorylated by Aurora A during mitosis. Its phospho-null mutant caused short metaphase spindles coupled with low microtubule flux rate. Interestingly, phosphorylation of TPX2 regulated its interaction with CLASP1 but not Kif2a. The effect of its mutant in shortening the spindle could be rescued by codepletion of CLASP1 and Kif2a that abolished microtubule flux. Together we propose that Aurora A–dependent TPX2 phosphorylation controls mitotic spindle length through regulating microtubule flux.

Introduction

Proper formation and function of a mitotic spindle guarantees an even distribution of chromosomes between daughter cells. A metaphase spindle maintains certain length, although polymerization constantly happens at the plus ends of the spindle microtubules (MTs) and depolymerization at the minus ends (Kwok and Kapoor, 2007). This balance is achieved mainly via CLASPs and a Kinesin-13 family protein Kif2a (Maiato et al., 2003, 2005; Gaetz and Kapoor, 2004; Ganem and Compton, 2004; Laycock et al., 2006; Maffini et al., 2009), along with a few other regulators of MT dynamics (Goshima et al., 2005; Buster et al., 2007; Kwok and Kapoor, 2007). TPX2 was characterized as an important MT-associated protein involved in the chromosome-dependent spindle assembly (Gruss et al., 2001, 2002; Schatz et al., 2003; Tsai et al., 2003). During mitosis, high concentrations of RanGTP in the vicinity of chromosomes dissociate TPX2 from the inhibition of importin α/β (Gruss et al., 2001; Tsai et al., 2003; Clarke and Zhang, 2008). Free TPX2 binds and activates Aurora A, an important kinase for centrosome function and spindle assembly (Kufer et al., 2002; Eyers et al., 2003; Tsai et al., 2003; Eyers and Maller, 2004; Fu et al., 2007). TPX2 possesses a strong ability to nucleate MTs (Schatz et al., 2003; Brunet et al., 2004). It, together with RanGTP, was found to stimulate the MT-dependent MT nucleation in *Xenopus laevis* egg extracts (Petry et al., 2013). Despite the efforts to explore TPX2 functions in multiple systems, elucidating its function has been challenging, as both depletion and overexpression result in similar multiple defects, including spindle collapse and multipolarity (Garrett et al., 2002; Gruss et al., 2002; Bird and Hyman, 2008; Eckerdt et al., 2008).

In this work, we reveal that TPX2 takes a unique role in coordinating MT polymerization/depolymerization to maintain metaphase spindle length. We find that TPX2 is phosphorylated by Aurora A and is essential for normal MT flux on the metaphase spindle. The effect of the phospho-null TPX2 in shortening the spindle could be rescued by removing both CLASP1 and Kif2a that abolishes the MT flux. Thus TPX2 phosphorylation regulates mitotic spindle length through the MT flux.

Results and discussion

Phosphorylation of TPX2 by Aurora A is required for normal spindle length

To address how TPX2 regulates spindle assembly, we collected asynchronous and mitotic HeLa cell lysates to investigate its posttranslational modifications. We observed robust elevation in the expression level of endogenous TPX2 in mitosis and a slight upward band shift on the gel indicating possible modifications (Fig. 1 A). The band shift was abolished when the mitotic lysate

*J. Fu and M. Bian contributed equally to this paper.

Correspondence to Chuanmao: Zhang zhangcm@pku.edu.cn

Abbreviations used in this paper: MT, microtubule.

The Rockefeller University Press $30.00
J. Cell Biol. Vol. 210 No. 3 373–383
www.jcb.org/cgi/doi/10.1083/jcb.201412109

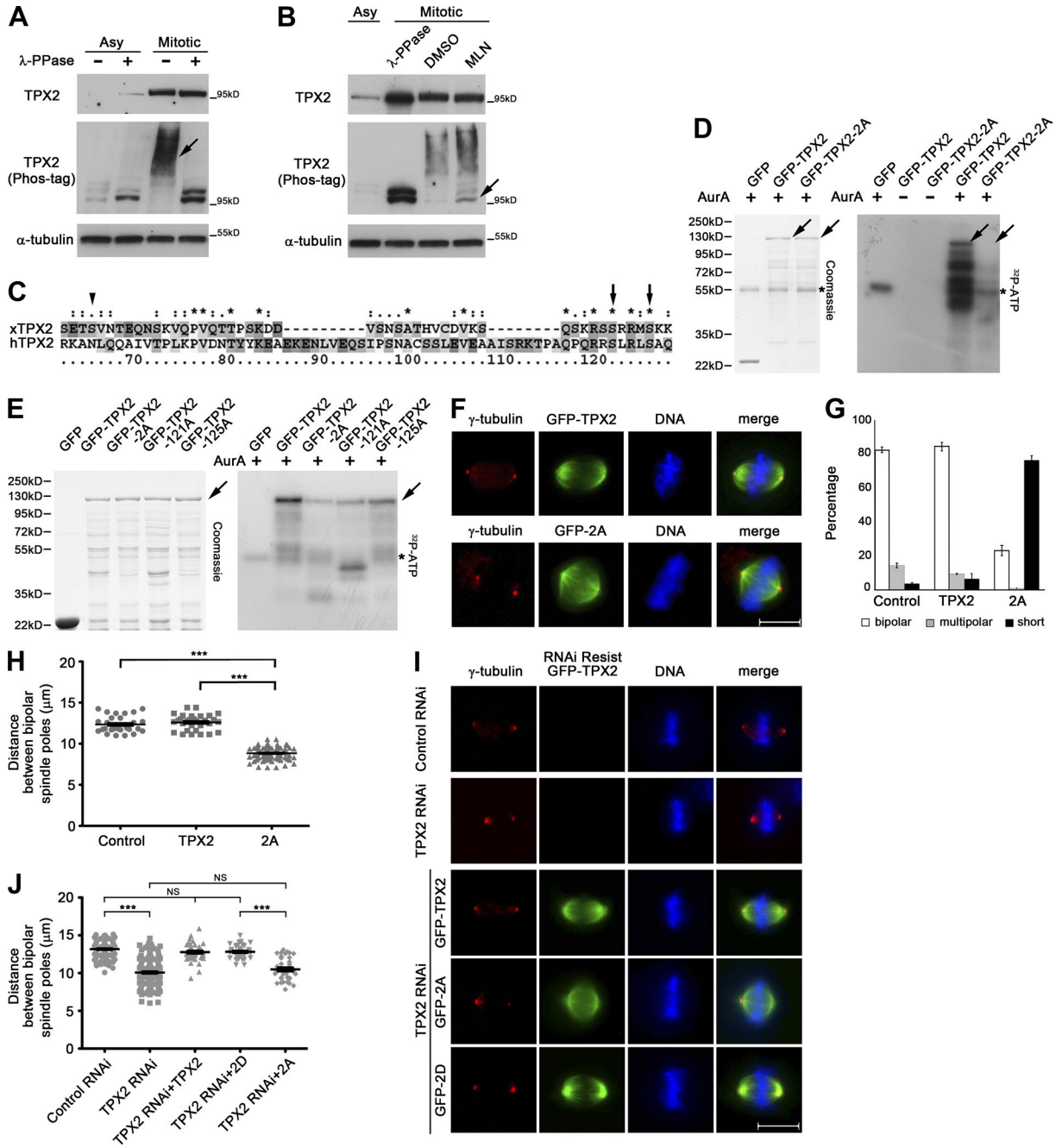

Figure 1. **TPX2 phosphorylation by Aurora A is required for normal spindle length.** (A) Asynchronous or mitotic HeLa cell lysates were treated with λ-phosphatase. In the middle panel, Mn^{2+}-phos-tag was introduced into the gel to enhance mobility shifts of phosphorylated TPX2. The majority of TPX2 is phosphorylated during mitosis (arrow). (B) Mitotic cell lysates were treated with λ-phosphatase, DMSO, or Aurora A inhibitor MLN8237 (MLN), and asynchronous cell lysate was left untreated (left lane). Nonphosphorylated TPX2 accumulates after Aurora A inhibition (arrow) compared with DMSO treatment. (C) Protein sequences of Human and *Xenopus* TPX2 were aligned by ClustalW and potential phosphorylation sites by Aurora A are indicated with arrows (conserved in both sequences) or an arrowhead (unique to *Xenopus* TPX2). Asterisks indicate positions that have identical residues on both sequences, double dots indicate highly conserved residues, and single dots indicate weakly conserved groups. (D and E) In vitro kinase assay using recombinant TPX2 as substrate. Phosphorylation of TPX2 is abolished after double serine-to-alanine mutation, and both S121 and S125 contribute to the phosphorylation. TPX2 is indicated by arrows and Aurora A by asterisks. (F–H) HeLa cells were transfected with GFP-TPX2 or -2A. Note that GFP-2A causes short bipolar spindles. Bar, 10 μm. 400 cells from three independent experiments were measured in G, and error bars indicate SD. Three independent experiments were performed in H: $n = 30$, 30, and 76. Error bars indicate SEM; ***, $P < 0.001$. (I and J) Isogenic stable HeLa cell lines were depleted of endogenous TPX2 and induced to express RNAi-resistant GFP-TPX2-WT, -2A, and -2D for 48 h. The distance between bipolar spindle poles was measured. Whereas WT- and 2D-expressing cells assemble spindles with normal length, 2A expression causes shorter bipolar spindles. Three independent experiments were performed in J: $n = 126$, 145, 39, 39, and 35. Error bars indicate SEM. ***, $P < 0.001$.

was pretreated by λ-phosphatase, suggesting that TPX2 was phosphorylated. We confirmed this by analyzing equivalent aliquots of the samples on a gel incorporating Mn^{2+}-phos-tag to bind phospho-proteins and reduce their mobility. It showed that most of TPX2 was phosphorylated during mitosis (Fig. 1 A).

We then looked for the kinase responsible for TPX2 phosphorylation. Previous reports have shown that TPX2 is phosphorylated by Aurora A in vitro (Kufer et al., 2002; Eyers et al., 2003; Eyers and Maller, 2004) and in a computational screen (Sardon et al., 2010). We therefore arrested HeLa cells in mitosis, treated them with Aurora A inhibitor MLN8237, and found that nonphosphorylated TPX2 accumulated (Fig. 1 B). This showed that phosphorylation of TPX2 in vivo depends on the kinase activity of Aurora A. Nevertheless, the phosphorylation of TPX2 was not completely abolished, indicating that some other kinases are involved.

In searching the potential Aurora A phosphorylation sites for the consensus sequence [K/R]X[S/T][AFILMV] (Ferrari et al., 2005; Ohashi et al., 2006), five serine/threonine residues were identified in human TPX2, of which only two are conserved from human to *Xenopus* (Fig. 1 C, arrows). Double and single mutations were made to confirm that TPX2-2A (S121/125A) could hardly be phosphorylated by Aurora A in vitro (Fig. 1 D), and both serine residues contributed to the proper phosphorylation (Fig. 1 E). This is in accord with a phosphoproteomics study that identified S121 and S125 as potential phosphorylation sites for Aurora A in mitotic HeLa cells (Kettenbach et al., 2011).

To determine the biological importance of TPX2 phosphorylation, we expressed the GFP-tagged TPX2-WT or -2A in HeLa cells. While the exogenous TPX2 caused a small amount of multipolar and short bipolar spindles, TPX2-2A showed a remarkable dominant-negative effect in generating short bipolar spindles (Fig. 1, F and G). The mean distance between spindle poles was reduced to 8.4 µm compared with the normal length of 12.3 µm (Fig. 1 H). We then established isogenic stable HeLa cell lines using the Flp-In T-REx system, which allows tetracycline-inducible expression of GFP-tagged TPX2-WT, -2A, and -2D (all containing synonymous mutations resistant to siRNA suppression) from a specific genomic location. Quantification of native GFP fluorescence in single mitotic cells and its proportion on spindle MTs showed that the expression levels of GFP-TPX2-WT, -2A, and -2D were comparable and that they were recruited to the spindle similarly (Fig. S1, A and B). TPX2 was depleted from these cells (Fig. S1 C) while the exogenous proteins were induced to express. The cells were synchronized in prometaphase by thymidine followed by Eg5 inhibitor, STLC, and then released into medium containing MG132 to allow full establishment of the bipolar spindles. We observed four categories of spindle phenotypes after TPX2 knockdown, as described previously (Gruss et al., 2002; Kufer et al., 2002; Bird and Hyman, 2008): first and most dominantly, spindle poles collapsed and two asters formed without organizing into bipolar structures; second, prometaphase-like spindles with two poles not fully separated and chromosomes not properly aligned; third, short bipolar spindles with chromosomes aligned at the equator; and fourth, multipolar spindles. Expression of GFP-TPX2-WT, -2A, or -2D could rescue most of the phenotype for collapsed poles and restore bipolarity (Fig. S1 D). However, bipolar spindles in the 2A-expressing cells were shorter compared with control, WT, or 2D-expressing cells (Fig. 1, I and J; and Videos 1–3). We also observed a small increase in the mitotic index when cells were depleted of endogenous TPX2 and expressing 2A (7.9%, compared with 5.3% in control, 5.2% in cells expressing WT, and 5.5% in 2D). This could be largely accounted for by the increase of cell population in prometaphase (3.8%, compared with 1.8% in control, 1.9% in cells expressing WT, and 2.2% in 2D), indicating that TPX2-2A causes a slightly prolonged early mitosis. Together our results show that phosphorylation of TPX2 by Aurora A is required for normal spindle length.

TPX2 phosphorylation rescues the short spindle phenomenon caused by Aurora A depletion

We then asked whether TPX2 functions downstream of Aurora A, or rather affects Aurora A in a feedback loop. Immunoprecipitation showed that GFP-TPX2-WT and -2A had similar affinity to Aurora A (Fig. S1 E), indicating that the interaction is independent of TPX2 phosphorylation. Then we depleted endogenous Aurora A and transiently expressed different TPX2 constructs (Fig. 2 A). Loss of Aurora A caused a 47% decrease in the mitotic index consistent with a previous report that Aurora A RNAi cells enter mitosis less efficiently (Hirota et al., 2003). We observed in 40% of metaphase cells a decrease in the spindle length upon Aurora A depletion (Fig. 2, B and C; Bird and Hyman, 2008). Expression of exogenous TPX2-WT or -2A did not rescue the phenomenon; however, TPX2-2D, a phospho-mimic mutant, restored the spindle length (Fig. 2, B and C). Together our data suggest that TPX2 is the main Aurora A target that regulates the spindle length.

We asked how TPX2 affects the spindle length. Recent reports showed that TPX2 interacts with Eg5 and facilitates the centrosome separation in early mitosis (Eckerdt et al., 2008; Ma et al., 2011; Gable et al., 2012). We found that TPX2-2A and -2D showed no preference in binding Eg5, although both were 41% less strong than WT (Fig. S1, F and G). The spindle localization of Eg5 was not affected by expression of TPX2 or its mutants (Fig. S1, H and I). These led us to propose that TPX2 phosphorylation regulates spindle length through another pathway. To ask which exact stage of spindle assembly is affected, we took advantage of an 11–amino acid peptide derived from the TAT protein transduction domain that can direct the efficient uptake of fusion proteins across the cell membrane within minutes (Liu et al., 2009). To test whether TPX2 affects the metaphase spindle independent of its role on centrosome separation, we synchronized the U2OS cells using double thymidine block and the Eg5 inhibitor STLC to induce monopolar spindle formation. These cells were then released into medium containing MG132 to allow full establishment of bipolar spindles before incubation with recombinant TAT-RFP-TPX2-WT, -2A, or -2D (Fig. 2, D and E). Compared with the normal spindle length of 12.2 µm, TPX2-2A decreased the distance between spindle poles to 10.1 µm, whereas WT and 2D barely had any effect (Fig. 2, F and G). These data show that TPX2 phosphorylation is necessary for maintaining the spindle length after the spindle reaches its steady state.

Phospho-null TPX2 inhibits MT flux on metaphase spindle

MT flux has been implicated as a major event in maintaining spindle length at later stages of mitosis (Laycock et al., 2006; Buster et al., 2007; Maffini et al., 2009). Based on our observations above, we tested whether TPX2 affects the rate of tu-

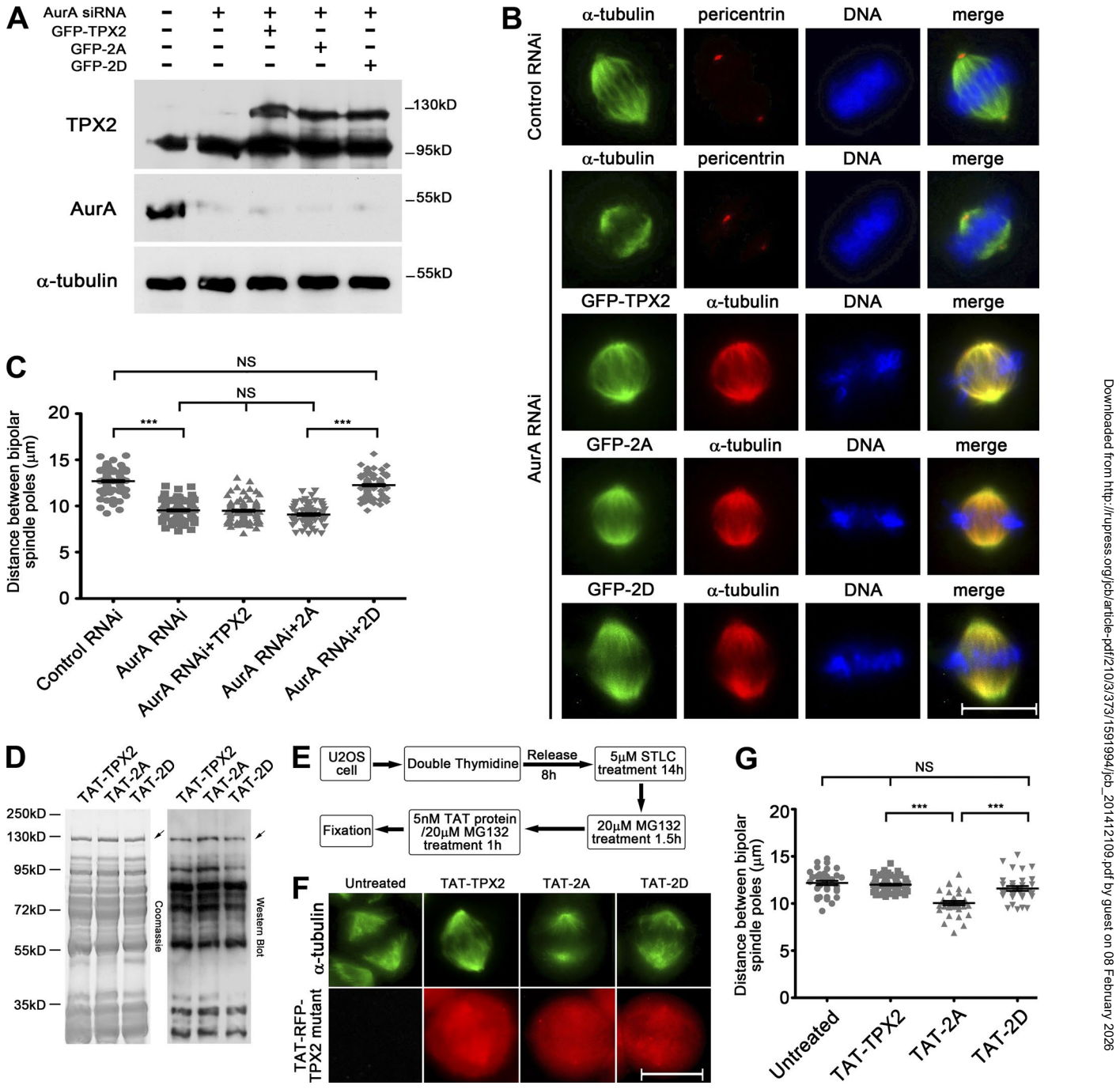

Figure 2. **TPX2 phosphorylation rescues the short spindle defect caused by Aurora A depletion and specifically affects spindle length in metaphase.** (A–C) HeLa cells were transfected with scrambled or Aurora A siRNA, or cotransfected with Aurora A siRNA and the indicated GFP-TPX2 constructs. Aurora A depletion causes short spindles, and TPX2-2D, but not -WT or -2A, could rescue such a defect. Bar, 10 μm. Three independent experiments were performed in C and n = 100, 94, 94, 60, and 88. Error bars indicate SEM. ***, $P < 0.001$. (D) His-TAT-RFP tagged TPX2-WT, -2A, and -2D purified from bacteria were visualized by Coomassie blue staining (left) and Western blotting with TPX2 antibody (right). The arrows indicate main bands of TPX2. (E–G) Cells treated with TAT-RFP-TPX2-2A show reduced length of metaphase spindles compared with normal structures in untreated, WT, or 2D-treated cells. Bar, 10 μm. n = 34, 76, 34, and 32. Error bars indicate SEM.

bulin dimers moving along the spindle MTs. We cotransfected U2OS cells with photoactivatable (PA) GFP-tagged α-tubulin and different mCherry-TPX2 constructs. In a time-lapse manner, we activated a rectangular region of PAGFP–α-tubulin near the chromosomes and tracked its movement (Fig. 3, A–C; and Videos 4–6). In the background of endogenous TPX2, when expressing either mCherry-tagged TPX2-WT or -2D, the tubulin dimers showed clear poleward flux at the rate of 1.0 ± 0.2 μm/min, whereas when expressing 2A, the velocity of MT flux was greatly reduced to 0.16 ± 0.12 μm/min (Fig. 3, D–F). Together, these show that phosphorylation of TPX2 is necessary for the MT flux on metaphase spindle.

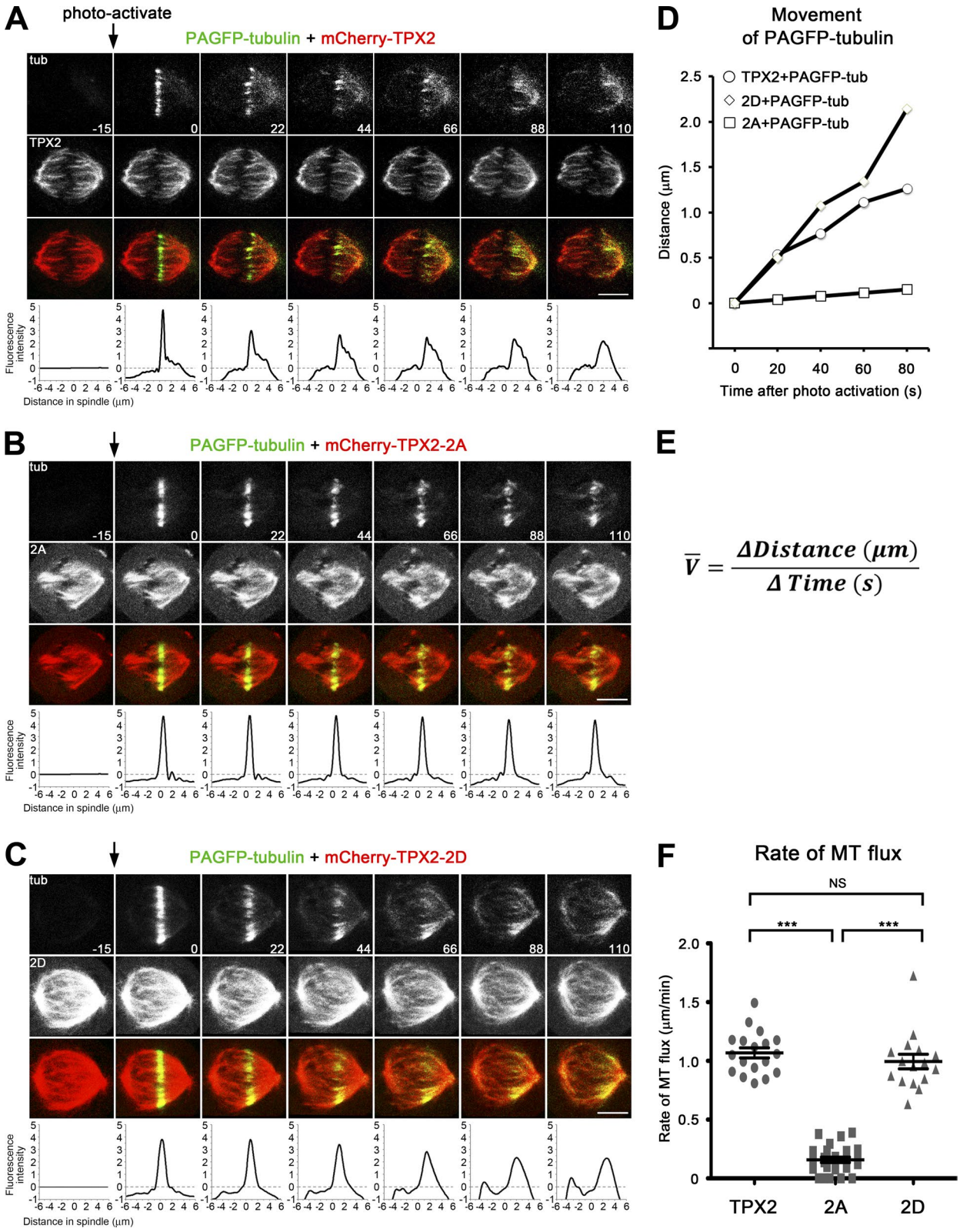

Figure 3. **Phospho-null TPX2 inhibits MT flux on metaphase spindles.** (A–D) U2OS cells were cotransfected with photoactivatable GFP-tagged α-tubulin (PAGFP-tubulin) and mCherry-TPX2, -2A, or -2D. GFP signal in a rectangular region near the MT plus ends was activated (time point 0, arrows) and tracked every 15 s. Representative time-course images are shown in A–C and fluorescence intensity profiles are plotted at the bottom. Bars, 5 μm. The x coordinate of the maximum intensity from each frame (≥ time 0) is shown in D. (E and F) The mean velocity of MT flux is defined by the ratio between distance relative to the equator and time. *n* in F: 18, 25, and 16. Error bars indicate SEM. ***, $P < 0.001$.

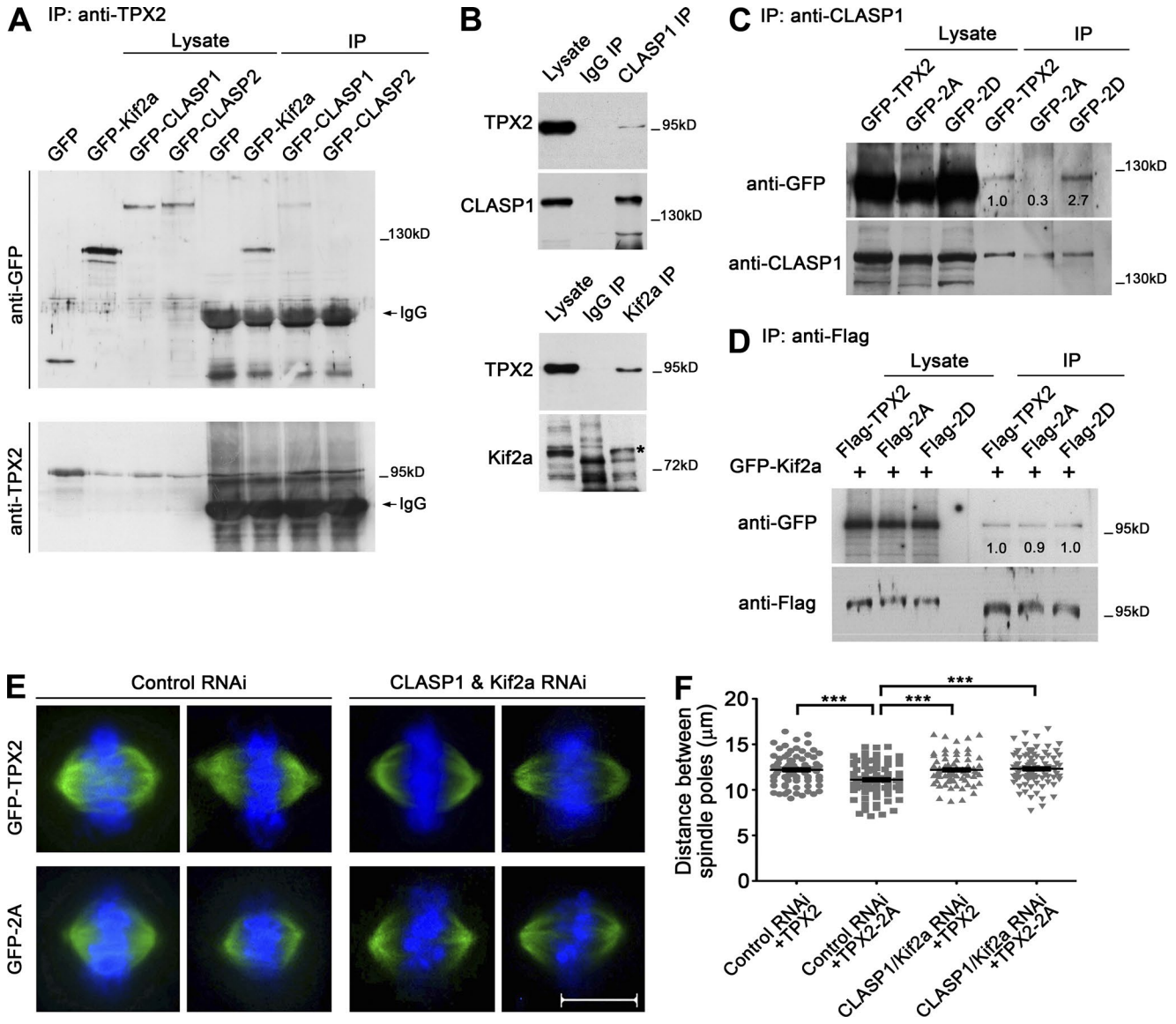

Figure 4. **TPX2 interacts with CLASP1 in a phospho-dependent manner, and its function in scaling spindle is bypassed by codepletion of CLASP1 and Kif2a.** (A) Mitotic HeLa cells transfected with the indicated constructs were immunoprecipitated with TPX2 antibody. Kif2a and CLASP1 form complexes with TPX2, whereas CLASP2 and GFP could not. (B) Mitotic HeLa lysates were immunoprecipitated with IgG, CLASP1, or Kif2a antibody. CLASP1 and Kif2a specifically bind to TPX2. The asterisk indicates Kif2a. (C) Mitotic cells transfected with GFP-tagged TPX2 constructs were immunoprecipitated with CLASP1 antibody. TPX2-2A binds significantly less CLASP1 than -WT and -2D. (D) Mitotic cells cotransfected with GFP-Kif2a and Flag-tagged TPX2 constructs were immunoprecipitated with flag antibody. TPX2, 2A, and 2D show similar affinity to Kif2a. (E and F) HeLa cells co-depleted of CLASP1/Kif2a were transfected with GFP-TPX2 or -2A. In mock-depleted cells, overexpression of TPX2-2A causes short spindles whereas in CLASP1/Kif2a-depleted cells, it does not affect the spindle length. Bar, 10 µm. *n* = 81, 89, 73, and 86. Error bars indicate SEM. ***, P < 0.001.

TPX2 phosphorylation regulates its interaction with CLASP1 but not Kif2a

We next asked how TPX2 might affect MT flux. We therefore expressed GFP-tagged CLASP1, CLASP2, or Kif2a in HeLa cells and pulled down endogenous TPX2 from mitotic lysates. We found that TPX2 specifically interacted with GFP-CLASP1 and -Kif2a (Fig. 4 A). In a parallel experiment, we pulled down endogenous CLASP1 and Kif2a from mitotic HeLa lysate and found that CLASP1 and Kif2a formed a complex with endogenous TPX2 (Fig. 4 B). Immunoprecipitation of either one of the three proteins always pulled down the other two, suggesting that they might be in a complex (Fig. S1 L). To test if these interactions reflect direct binding, we purified recombinant GST-tagged CLASP1 and Kif2a, mixed with recombinant His-GFP-tagged TPX2, and performed in vitro GST pull-down. This revealed that CLASP1 and Kif2a directly bound to TPX2 (Fig. S1 K).

We then examined whether TPX2 phosphorylation affects these interactions using three approaches. First, we transfected cells with GFP-tagged TPX2-WT, -2A, or -2D and pulled down endogenous CLASP1. This showed that CLASP1 bound to less TPX2-2A than -WT and -2D (Fig. 4 C). We also cotransfected cells with GFP-Kif2a and Flag-tagged TPX2-WT, -2A, or -2D, and performed immunoprecipitation using Flag antibody. This showed that Kif2a bound to TPX2-WT, -2A, and -2D with similar affinity (Fig. 4 D). In a second approach, we transfected cells with GFP-CLASP1 or -Kif2a, treated them with MLN8237 for 30 min, and performed immunoprecipitation using GFP antibody. This showed that CLASP1 pulled down less and that

Kif2a pulled down a similar amount of TPX2 in the presence of MLN8237 (Fig. S1 J). Finally, we performed in vitro GST pull-down where we mixed GST-tagged CLASP1 or Kif2a with His-GFP–tagged TPX2-WT, -2A, or -2D. This revealed that there was less affinity of CLASP1 to TPX2-2A (Fig. S1 K); Kif2a appeared to bind more TPX2-2A than -WT and -2D (Fig. S1 K), in contrast to our immunoprecipitation experiment that failed to reveal any difference (Fig. 4 D and Fig. S1 J). One reason for the discrepancy could be that the in vitro system did not fully represent what happened in the cell lysate. Nevertheless, these data show that the interaction between TPX2 and the MT flux factor CLASP1 is Aurora A phosphorylation–dependent and that abolishing TPX2 phosphorylation reduces its affinity to CLASP1.

TPX2 phosphorylation regulates spindle length through MT flux

The above result that phosphorylation of TPX2 increased its affinity to CLASP1 but not Kif2a led us to hypothesize that TPX2 phosphorylation might be important to maintain the balance between MT polymerization and depolymerization. To test this, we co-depleted CLASP1 and Kif2a while transiently expressing TPX2-2A in HeLa cells. Previous reports have shown that depletion of CLASP1 or Kif2a results in short/monopolar spindles in human cells; but if both are depleted, the spindle remains normal length (Ganem and Compton, 2004; Maffini et al., 2009). This functional cooperation is also seen in *Drosophila* S2 cells (Laycock et al., 2006; Buster et al., 2007). We confirmed that upon double knockdown of CLASP1 and Kif2a, there was no obvious MT flux on the metaphase spindle, as previously reported (Fig. S2, A and B; Buster et al., 2007; Maffini et al., 2009). Under this condition, TPX2-2A could no longer show the dominant-negative effect of generating short spindles (Fig. 4, E and F). This result suggests that TPX2 phosphorylation is required for normal spindle length through regulating MT flux. Expression of TPX2-2A greatly restored the spindle bipolarity upon Kif2a depletion (Fig. S2 C), which is reminiscent of CLASP1 knockdown (Ganem and Compton, 2004; Maffini et al., 2009). This suggests that TPX2 phosphorylation positively regulates the function of CLASP1.

Phosphorylation of TPX2 by Aurora A is important for spindle organization in *Xenopus* extracts

To address the conservation of the above Aurora A–TPX2 pathway, we used similar strategies in mitotic *Xenopus* egg extracts. First, two serine residues in *Xenopus* TPX2 sequence (xTPX2, S90 and S94) corresponding to the S121/125 of human TPX2 were mutated. Another serine (S48), which is not conserved in human TPX2, was also included based on a previous report (Fig. 1 C; Eyers and Maller, 2004). The incorporation of labeled ^{32}P into xTPX2-3A was greatly reduced (Fig. S3, A and B), and deletion of the xTPX2-pEg2 interacting domain (aa 1–39 of xTPX2) did not affect the phosphorylation of xTPX2 in vitro (Fig. S3, A and C). The GFP-tagged recombinant xTPX2-WT, -3A, and -3D were subsequently subjected to functional analysis in mitotic *Xenopus* egg extracts that had been depleted of pEg2 or xTPX2 (Fig. 5, A and B). In the mock-depleted extract, we observed bipolar spindles and a small proportion of other structures including asters and abnormal spindles with fewer MTs or unfocused poles. Depletion of xTPX2 caused a significant decrease in the percentage of bipolar spindles, which could be rescued by adding back recombinant xTPX2-WT and -3D but not -3A (Fig. 5, C and D). Similarly, the effects of pEg2 depletion could only be rescued by pEg2 itself or xTPX2-3D, but not xTPX2-WT or -3A (Fig. 5, C and D). These results indicate that the Aurora A–dependent phosphorylation of TPX2 is a conserved mechanism to regulate bipolar spindle assembly.

Our study reveals a novel function of TPX2 in scaling the spindle in later stage of mitosis when the spindle reaches a steady state (Fig. S2 D). This function of TPX2 is under the regulation of Aurora A phosphorylation on two conserved serine residues, the role of which has not been studied. We found that TPX2 interacts with MT flux factors CLASP1 and Kif2a. The affinity of TPX2 to CLASP1 is phospho-dependent, yet this is not the case for the TPX2–Kif2a interaction. It is therefore tempting to speculate that the phosphorylation of TPX2 regulates the activity of CLASP1 via a not-yet-known mechanism, and this could affect the activity of CLASP1 in incorporating tubulin dimers at the plus end of the spindle MTs. Both depletion of CLASP1 and expression of TPX-2A restore the spindle bipolarity upon Kif2a knockdown, suggesting that TPX2 phosphorylation positively regulates CLASP1. TPX2 might have an effect on Kif2a since they interact directly, but this is likely not to be affected by its phosphorylation state. Therefore, loss of phosphorylation in the mutant TPX2 may destroy the balance between MT polymerization and depolymerization, resulting in slow MT flux and short spindles. The N terminus of CLASP1 causes multiple dominant-negative defects in mitotic *Xenopus* extracts including hollow, enlarged, and multipolar spindles (Patel et al., 2012), which are reminiscent of our observations after xTPX2 depletion. Kif2a was shown to drive the spindle scaling during *Xenopus* embryogenesis through the fluctuation of its MT-destabilizing activity (Wilbur and Heald, 2013). These observations could possibly reflect the same pathway. Of course we could not rule out the possibility that other factors affecting MT flux might also be regulated by TPX2 phosphorylation. For instance, Kinesin-13 family members MCAK (Ganem et al., 2005) and KLP59C, Kinesin-8 KLP67A, and MT polymerization factor Dis1/Msps/XMAP215/TOG (Buster et al., 2007), as well as dynein, which can promote the poleward streaming of CLASP in *Drosophila* (Reis et al., 2009). Therefore, future work needs to study how phosphorylation of TPX2 regulates CLASP1 and whether it has impacts on other factors listed above, in order to understand how TPX2 regulates MT flux and the metaphase spindle length.

Our study and others have suggested that the role of TPX2 in scaling the spindle might be conserved during evolution. In *C. elegans*, TPXL-1 RNAi shows a strong effect on reducing the spindle length; the protein amounts at the centrosome and its gradient decay length along MTs are proportional to the spindle length (Greenan et al., 2010). In *Xenopus tropicalis* egg extracts where chromosome-induced spindles are smaller than those in *Xenopus laevis*, TPX2 is threefold more abundant (Helmke and Heald, 2014). It would be interesting to test whether the phosphorylation of TPX2 by Aurora A also plays similar role in these organisms. Nevertheless, *Drosophila* might be an exception because TPX2 homologue has almost no effect on mitosis in S2 cells (Goshima, 2011). Collectively, our study shows that TPX2 phosphorylation by Aurora A is responsible for maintaining metaphase spindle length by regulating the MT flux in human cells. This process is important for the later chromosome separation and the faithful cell division.

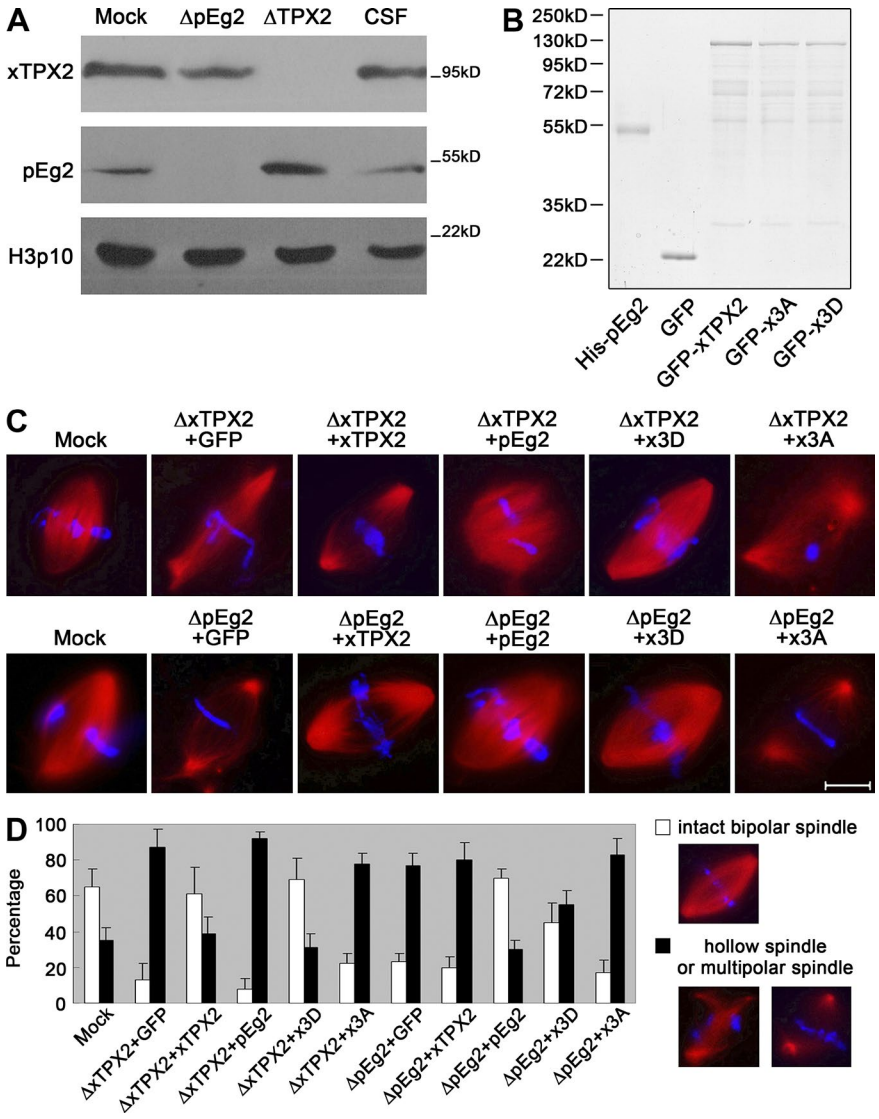

Figure 5. **TPX2 phosphorylation by Aurora A is required for intact bipolar spindle assembly in mitotic *Xenopus* egg extract.** (A) Mitotic extracts (CSF) depleted of pEg2 (Aurora A) or xTPX2 were subjected to Western blotting. Histone H3 Serine10 phosphorylation serves as a mitotic marker. (B) Coomassie blue staining showing the recombinant proteins added in C. (C and D) CSF depleted of xTPX2 or pEg2 was added with indicated proteins. Sperm-induced bipolar spindle formation was impaired by xTPX2 or pEg2 depletion. Among all proteins to rescue such defects, GFP-xTPX2-3D showed the best effect, whereas GFP and GFP-xTPX2-3A showed no rescue. GFP-xTPX2 could partially rescue xTPX2 but not pEg2 depletion; His-pEg2 could rescue pEg2 but not xTPX2 depletion. Bar, 20 µm. Three independent experiments were performed in D, each measuring 100 spindles. Error bars indicate SD.

Materials and methods

Molecular cloning, protein purification, and antibody preparation

GFP-CLASP1 and -CLASP2 constructs were provided by H. Maiato (Institute for Molecular Cell Biology, Porto, Portugal), and GFP-Kif2a construct was provided by G. Fang (Genentech, San Francisco, CA) and C.-Y. Jang (Sookmyung Women's University, Seoul, South Korea). Human *Aurora A* and *TPX2* were cloned by RT-PCR from HeLa cell lysate as described previously (Fu et al., 2009). *Xenopus pEg2* and *xTPX2* were cloned from a cDNA library of *Xenopus* oocytes (Takara Bio Inc.). Mutants and truncates of *TPX2*/*xTPX2* were generated by PCR with specific primers. For overexpression in HeLa cells, *TPX2* cDNAs were cloned into pEGFP-C1 (6084-1; Takara Bio Inc.) or p3×-FLAG-CMV vector (E4026; Sigma-Aldrich) using BamHI–SalI on the cDNAs and BglII–SalI on the vectors. To obtain recombinant proteins, *TPX2* cDNAs were inserted into pET28a (69864-3; EMD Millipore) using SalI–HindIII, *xTPX2* using EcoRI–SalI, and *pEg2* using BamHI–XhoI, and expressed in *E. coli* BL21 (DE3 pLys). Based on the need of the individual experiment, either GFP was fused to the N terminus of the *TPX2* cDNAs to increase protein stability (Brunet et al., 2004), or TAT-RFP was introduced to enable instant absorption by the cells. All proteins were affinity purified using Ni-NTA agarose (for His-tagged proteins; QIAGEN) or Glutathione Sepharose 4B beads (for GST-tagged proteins; GE Healthcare), according to the manufacturers' protocol. Antibodies against GFP, Aurora-A, and TPX2 were raised in both rabbits and mice using His-tagged full-length proteins as described previously (Fu et al., 2009); antibodies against pEg2 and xTPX2 were raised in rabbits using His-tagged full-length proteins, and Kif2a and CLASP1 in mice, using GST-tagged Kif2a 1–95 aa and CLASP1 1239–1538 aa, respectively. Other antibodies were as follows: mouse anti-flag (F1804; Sigma-Aldrich), rabbit anti–γ-tubulin (T3320; Sigma-Aldrich), mouse anti–α-tubulin (T9026; Sigma-Aldrich), rabbit anti-pericentrin (ab4448; Abcam); rabbit anti-actin (sc-130656; Santa Cruz Biotechnology, Inc.), mouse anti-Eg5 (611187; BD), mouse anti–phospho-histone H3 (Ser-10; 05-806, EMD Millipore), rabbit anti-TPX2 (12245; Cell Signaling Technology), and rabbit anti-Kif2a (HPA004716; Sigma-Aldrich), Alexa Fluor 488 donkey anti–mouse, Alexa Fluor 546 donkey anti–mouse, and Alexa Fluor 546 donkey anti–rabbit (all from Invitrogen). Goat anti–rabbit/mouse IgG HRP was from Jackson ImmunoResearch Laboratories, Inc.

Cell synchronization, siRNA and plasmid transfections, and cell line establishment

HeLa or U2OS cells were cultured in DMEM supplemented with 10% bovine calf serum, 100 U/ml penicillin, and 100 µg/ml streptomycin (all from Hyclone; GE Healthcare) at 37°C and 5% CO_2. To be synchro-

nized in mitosis for immunoprecipitation, HeLa cells were treated with double thymidine, released for 8 h, and supplemented with 50 ng/ml nocodazole for another 6 h. To be synchronized in metaphase for immunofluorescence (Fig. S1 D), HeLa cells were treated with thymidine for 24 h, released for 3 h, and incubated with 5 µM STLC for 8 h to induce monopolar spindle formation. These cells were then released into fresh medium containing 20 µM MG132 for 2 h to allow full establishment of bipolar spindles. To deliver siRNA and plasmid DNA, cells grown on coverslips were transfected using Lipofectamine 2000 (Invitrogen). The following sequences were used: Aurora A, 5′-UUCUUAGACUGUAUGGUUA-3′ (GE Healthcare); TPX2, 5′-CCAGUUGACAACACUUACU-3′; CLASP1, 5′-GCCAUUAUGCCAACUAUCU-3′ (Mimori-Kiyosue et al., 2005); Kif2a, 5′-GGCAAAGAGAUUGACCUGG-3′ (Ganem and Compton, 2004); and negative control, 5′-UUCUCCGAACGUGUCACGU-3′. For making TPX2 RNAi-resistant mutants, 5′-CCGGTCGATAATACGTATTACAAAGAGGCA-3′ and 5′-TGCCTCTTTGTAATACGTATTATCGACCGG-3′ were used.

To establish tetracycline-inducible cell lines for expressing GFP-TPX2-WT, -2A, and -2D, Flp-In T-REx host HeLa cell lines (Shrestha et al., 2014) were cotransfected with pOG44 and a Gateway vector (Torres et al., 2009) containing GFP-TPX2-WT, -2A, or -2D (all containing synonymous mutations resistant to siRNA suppression) under the control of CMV/TetO_2 promoter and FRT recombinant site. Homologous recombination between FRT sites in the Gateway vector and on the host cell chromosome, catalyzed by the Flp recombinase expressed from pOG44, generated the derivative cell lines into which the gene had been stably integrated into the host cell chromosome. These cells were then selected and maintained using the puromycin resistance (Life Technologies) acquired as a consequence of the recombination event. Next, single colonies were sorted using FACS and tested for the expression levels upon tetracycline induction. The ones that expressed comparable amount of GFP-TPX2-WT, -2A, and -2D were used for experiments. To avoid leaking expression of the exogenous proteins, cells were cultured in DMEM supplemented with 10% qualified FBS (Life Technologies).

TAT fusion protein treatment

U2OS cells were synchronized with double thymidine, released for 8 h, and incubated with 5 µM STLC for 14 h to induce monopolar spindle formation. These cells were then released into fresh medium containing 20 µM MG132 for 1.5 h to allow for full establishment of bipolar spindles. Finally, 5 nM of recombinant protein TAT-RFP-TPX2-WT, -2A, or -2D was added to the medium and the cells were incubated for 1 h before fixation.

λ-PPase treatment and phos-tag gel electrophoresis

Cells were collected from a 35-mm dish and rinsed twice with ice-cold HBS consisting of 20 mM Hepes, pH 7.4, and 150 mM NaCl. They were subsequently lysed on ice for 15 min with RIPA buffer, containing 1% NP-40, 50 mM Tris-HCl, pH 7.4, 150 mM NaCl, 0.5 mM EDTA, 0.5% sodium deoxycholate, 0.1% SDS, and complete EDTA-free protease inhibitors (Roche). Lysates were centrifuged at 20,000 *g* for 15 min, and supernatants were supplemented with 10× PMP buffer, 10× $MnCl_2$, and 400 U λ-PPase (New England Biolabs, Inc.). The reactions were kept at 30°C for 30 min before being quenched with SDS sample buffer. Phos-tag gel electrophoresis was performed according to the manufacturer's protocol (Wako Pure Chemical Industries). In brief, 8% separating gel was prepared with 25 µM Phos-tag Acrylamide AAL-107 and 50 µM $MnCl_2$. We then mixed thoroughly, allowed the gel to polymerize for 1 h, and prepared the normal stacking gel. Samples were run at low voltage around 60 V until the Bromophenol blue reached the bottom. The gel was then soaked in transfer buffer containing 1 mmol/liter EDTA for 10 min and transfer buffer without EDTA for another 10 min before transferring to PVDF membrane for antibody blotting.

Immunoprecipitation

Protein–A Sepharose beads (GE Healthcare) were washed three times with PBS, diluted into 500 µl, and incubated with indicated antibody in each experiment for 1 h at 4°C. Beads were then washed three times with lysis buffer, consisting of 0.5% NP-40, 20 mM Tris-HCl, pH 7.4, 500 mM NaCl, 0.5 mM EGTA, 10 mM NaF, 2 mM sodium vanadate, 10 mM β-glycerophosphate, 10 µg/ml leupeptin, 0.7 µg/ml pepstatin A, 1.5 µg/ml aprotinin, and 1 mM PMSF. For immunoprecipitation, mitotic HeLa cells transfected with the indicated constructs were shaken off the culture dish and lysed on ice for 30 min with lysis buffer. Lysates were centrifuged at 16,000 *g* for 15 min, and supernatants were incubated with beads for 1 h at 4°C on the rotator. After six washes with lysis buffer, the bound proteins were analyzed by Western blotting.

In vitro binding assay

Recombinant GST/GST-Kif2a/GST-CLASP1 and GFP/GFP-TPX2/GFP-2A/GFP-2D proteins were diluted to a final concentration of 1 mg/ml in PBS. 10 µg of GST-tagged and 30 µg of GFP-tagged proteins were mixed for each reaction in 500 µl PBS/0.1% Triton X-100 and rotated for 0.5 h at 4°C. Next, 20 µl of prewashed Glutathione Sepharose 4B beads (GE Healthcare) was added and the whole mixture was rotated for another 1.5 h at 4°C. Finally, the beads were spun down, washed four times with PBS/0.1% Triton X-100, boiled in 2× sample buffer, and analyzed by Western blotting analysis.

Immunofluorescence microscopy, live cell imaging, and statistical analysis

Cells grown on coverslips were fixed with precooled methanol for 6 min on ice. After rehydration in TBS, the cells were incubated with the primary antibody overnight at 4°C. Then they were washed three times in TBS and incubated with the secondary antibody for 45 min at room temperature. Coverslips were mounted onto slides by using Mowiol containing 1 µg/ml DAPI and analyzed under a microscope (Axiovert 200M; Carl Zeiss) equipped with a 63×/1.4 NA oil objective lens. Images were captured with a camera (MRM CCD; Carl Zeiss) and Axiovision image acquisition software. For live cell imaging, U2OS cells were cotransfected with photoactivatable GFP-tagged α-tubulin and different mutants of mCherry-TPX2 (Videos 4–6). Before imaging, cells were changed to CO_2-independent medium (18045-088; Life Technologies) supplemented with 200 mM L-glutamine and 10% FBS. Images were captured at 37°C under a confocal microscope (LSM 510 Meta; Carl Zeiss; 100×/1.4 NA oil objective lens, an AxioCam digital microscope camera, and LSM510 software). Bipolar spindles were selected according to the red channel (mCherry-TPX2) and the 405 nm laser was used to activate a rectangular region of PAGFP–α-tubulin signal near the chromosomes (time point = 0). The movement of the tubulin dimers was then tracked using 488/514 nm lasers every 15 s. Alternatively, HeLa cells cultured in DMEM supplemented with 10% FBS were tracked every 3 min with a microscope (ECLIPSE Ti; Nikon) at 37°C and in a 5% CO_2 environment (Videos 1–3). Images were captured with a 60×/1.4 NA oil objective lens, an EM CCD (Hamamatsu Photonics, Inc.), and Volocity software. To determine the spindle length, the distances between two spindle poles were measured by AxioVision LE software. The mean spindle length was determined from at least three independent experiments and graphed with the SEM using GraphPad Prism 5 software (GraphPad Software). Statistical significance was also analyzed for p-values using GraphPad Prism 5. To measure the fluorescence intensity of TPX2 or Eg5 in a single

cell or on a spindle, ImageJ was applied to select the region of the cell or spindle and the total fluorescence was calculated by the size of the area times the mean intensity that had been deducted from the background intensity. To determine the velocity of MT flux, spindles were first rotated to the horizontal position according to the red channel (mCherry-TPX2). Each frame from the same movie was then adjusted using ImageJ plugin StackReg to minimize the movement of the whole spindle. Next, the ImageJ macro Spindle Microtubule Frap/Flip Analyzer (http://cmci.embl.de/downloads/spindlefanalyzer; Ma et al., 2010) was applied. The macro uses the red channel to create a mask that specifies the area of the spindle, and then this specified area is measured for the integrated intensity profile of the green channel (projected in the y axis, and measured along the x axis). The profile was plotted in Excel after smoothed via B-spline and the x coordinate of the maximum intensity was exported to represent the position of the fluxing tubulin dimers. The velocity of MT flux was defined by the ratio between the distance relative to the equator and the time, and based on our observation it's mostly linear within the first 60 s. For this reason we always evaluated the mean velocity at time point = 60 s for the statistical data in Fig. 3 F.

Kinase assays

To test the phosphorylation of different TPX2 mutants, 1 µg of recombinant protein was incubated with 1 µg Aurora A (or pEg2) kinase for 20 min at 30°C. Kinase assays were performed in 50 mM Tris-HCl, pH 7.4, 50 mM NaCl, 10 mM $MgCl_2$, 1 mM DTT, and 100 µM ATP containing 3,000 Ci/mmol γ-[^{32}P]ATP. Reactions were quenched with SDS sample buffer and analyzed by SDS-PAGE and autoradiography.

Xenopus egg extract experiments

Xenopus CSF extracts were prepared as described previously (Fu et al., 2010). In brief, eggs were washed sequentially with XB (10 mM Hepes, 0.1 mM $CaCl_2$, 100 mM KCl, 1 mM $MgCl_2$, and 50 mM sucrose, pH 7.8) and CSF-XB buffer (10 mM Hepes, 2 mM $MgCl_2$, 0.1 mM $CaCl_2$, 100 mM KCl, 5 mM EGTA, and 50 mM sucrose, pH 7.8), and centrifuged in CSF-XB plus cytochalasin B (100 µg/ml) at 13,000 rpm for 10 min (TLS55 rotor; Beckman Coulter) to obtain the supernatant. To deplete pEg2 or xTPX2, protein A–conjugated Dynal beads were coupled with xTPX2 or pEg2 antibody, incubated with CSF on ice for 40 min, and removed by a magnet. We then repeated the process to make sure of full depletion. To analyze the rescue effects by different recombinant proteins, demembranated *Xenopus* sperms (600 nuclei/µl), Rhodamine-labeled tubulin, and these proteins were added to the extracts to allow spindle assembly for 45 min at 21°C. The samples were then fixed with fixation buffer (Marc's modified ringers [MMR] plus 4% paraformaldehyde and 50% glycerol) and analyzed under a microscope (Axiovert 200M; Carl Zeiss).

Online supplemental material

Fig. S1 shows the binding capacity of TPX2 phospho mutants to different interacting partners. Fig. S2 supports the data presented in Fig. 4 (E and F) and shows that TPX2 regulates metaphase spindle length through affecting MT flux. Fig. S3 shows that *Xenopus* TPX2 is phosphorylated by Aurora A. Video 1 shows spindle formation in the background of GFP-TPX2. Video 2 shows spindle formation in the background of GFP-TPX2-2A. Video 3 shows spindle formation in the background of GFP-TPX2-2D. Video 4 shows MT flux on metaphase spindles in the background of GFP-TPX2. Video 5 shows MT flux on metaphase spindles in the background of GFP-TPX2-2A. Video 6 shows MT flux on metaphase spindles in the background of GFP-TPX2-2D. Online supplemental material is available at http://www.jcb.org/cgi/content/full/jcb.201412109/DC1.

Acknowledgements

We thank Dr. Jing Wu (Tsinghua University, Beijing, China) for the data analysis of MT flux.

This work was supported by funds from the National Natural Science Foundation of China (91313302, 31071188, 31030044, 90913021, and 31371365) and the State Key Basic Research and Development Plan (2010CB833705 and 2014CB138402).

The authors declare no competing financial interests.

Submitted: 22 December 2014
Accepted: 29 June 2015

References

Bird, A.W., and A.A. Hyman. 2008. Building a spindle of the correct length in human cells requires the interaction between TPX2 and Aurora A. *J. Cell Biol.* 182:289–300. http://dx.doi.org/10.1083/jcb.200802005

Brunet, S., T. Sardon, T. Zimmerman, T. Wittmann, R. Pepperkok, E. Karsenti, and I. Vernos. 2004. Characterization of the TPX2 domains involved in microtubule nucleation and spindle assembly in *Xenopus* egg extracts. *Mol. Biol. Cell.* 15:5318–5328. http://dx.doi.org/10.1091/mbc.E04-05-0385

Buster, D.W., D. Zhang, and D.J. Sharp. 2007. Poleward tubulin flux in spindles: regulation and function in mitotic cells. *Mol. Biol. Cell.* 18:3094–3104. http://dx.doi.org/10.1091/mbc.E06-11-0994

Clarke, P.R., and C. Zhang. 2008. Spatial and temporal coordination of mitosis by Ran GTPase. *Nat. Rev. Mol. Cell Biol.* 9:464–477. http://dx.doi.org/10.1038/nrm2410

Eckerdt, F., P.A. Eyers, A.L. Lewellyn, C. Prigent, and J.L. Maller. 2008. Spindle pole regulation by a discrete Eg5-interacting domain in TPX2. *Curr. Biol.* 18:519–525. http://dx.doi.org/10.1016/j.cub.2008.02.077

Eyers, P.A., and J.L. Maller. 2004. Regulation of *Xenopus* Aurora A activation by TPX2. *J. Biol. Chem.* 279:9008–9015. http://dx.doi.org/10.1074/jbc.M312424200

Eyers, P.A., E. Erikson, L.G. Chen, and J.L. Maller. 2003. A novel mechanism for activation of the protein kinase Aurora A. *Curr. Biol.* 13:691–697. http://dx.doi.org/10.1016/S0960-9822(03)00166-0

Ferrari, S., O. Marin, M.A. Pagano, F. Meggio, D. Hess, M. El-Shemerly, A. Krystyniak, and L.A. Pinna. 2005. Aurora-A site specificity: a study with synthetic peptide substrates. *Biochem. J.* 390:293–302. http://dx.doi.org/10.1042/BJ20050343

Fu, J., M. Bian, Q. Jiang, and C. Zhang. 2007. Roles of Aurora kinases in mitosis and tumorigenesis. *Mol. Cancer Res.* 5:1–10. http://dx.doi.org/10.1158/1541-7786.MCR-06-0208

Fu, J., M. Bian, J. Liu, Q. Jiang, and C. Zhang. 2009. A single amino acid change converts Aurora-A into Aurora-B-like kinase in terms of partner specificity and cellular function. *Proc. Natl. Acad. Sci. USA.* 106:6939–6944. http://dx.doi.org/10.1073/pnas.0900833106

Fu, W., W. Tao, P. Zheng, J. Fu, M. Bian, Q. Jiang, P.R. Clarke, and C. Zhang. 2010. Clathrin recruits phosphorylated TACC3 to spindle poles for bipolar spindle assembly and chromosome alignment. *J. Cell Sci.* 123:3645–3651. http://dx.doi.org/10.1242/jcs.075911

Gable, A., M. Qiu, J. Titus, S. Balchand, N.P. Ferenz, N. Ma, E.S. Collins, C. Fagerstrom, J.L. Ross, G. Yang, and P. Wadsworth. 2012. Dynamic reorganization of Eg5 in the mammalian spindle throughout mitosis requires dynein and TPX2. *Mol. Biol. Cell.* 23:1254–1266. http://dx.doi.org/10.1091/mbc.E11-09-0820

Gaetz, J., and T.M. Kapoor. 2004. Dynein/dynactin regulate metaphase spindle length by targeting depolymerizing activities to spindle poles. *J. Cell Biol.* 166:465–471. http://dx.doi.org/10.1083/jcb.200404015

Ganem, N.J., and D.A. Compton. 2004. The KinI kinesin Kif2a is required for bipolar spindle assembly through a functional relationship with MCAK. *J. Cell Biol.* 166:473–478. http://dx.doi.org/10.1083/jcb.200404012

Ganem, N.J., K. Upton, and D.A. Compton. 2005. Efficient mitosis in human cells lacking poleward microtubule flux. *Curr. Biol.* 15:1827–1832. http://dx.doi.org/10.1016/j.cub.2005.08.065

Garrett, S., K. Auer, D.A. Compton, and T.M. Kapoor. 2002. hTPX2 is required for normal spindle morphology and centrosome integrity during vertebrate cell division. *Curr. Biol.* 12:2055–2059. http://dx.doi.org/10.1016/S0960-9822(02)01277-0

Goshima, G. 2011. Identification of a TPX2-like microtubule-associated protein in *Drosophila*. *PLoS ONE.* 6:e28120. http://dx.doi.org/10.1371/journal.pone.0028120

Goshima, G., R. Wollman, N. Stuurman, J.M. Scholey, and R.D. Vale. 2005. Length control of the metaphase spindle. *Curr. Biol.* 15:1979–1988. http://dx.doi.org/10.1016/j.cub.2005.09.054

Greenan, G., C.P. Brangwynne, S. Jaensch, J. Gharakhani, F. Jülicher, and A.A. Hyman. 2010. Centrosome size sets mitotic spindle length in *Caenorhabditis elegans* embryos. *Curr. Biol.* 20:353–358. http://dx.doi.org/10.1016/j.cub.2009.12.050

Gruss, O.J., R.E. Carazo-Salas, C.A. Schatz, G. Guarguaglini, J. Kast, M. Wilm, N. Le Bot, I. Vernos, E. Karsenti, and I.W. Mattaj. 2001. Ran induces spindle assembly by reversing the inhibitory effect of importin α on TPX2 activity. *Cell.* 104:83–93. http://dx.doi.org/10.1016/S0092-8674(01)00193-3

Gruss, O.J., M. Wittmann, H. Yokoyama, R. Pepperkok, T. Kufer, H. Silljé, E. Karsenti, I.W. Mattaj, and I. Vernos. 2002. Chromosome-induced microtubule assembly mediated by TPX2 is required for spindle formation in HeLa cells. *Nat. Cell Biol.* 4:871–879. http://dx.doi.org/10.1038/ncb870

Helmke, K.J., and R. Heald. 2014. TPX2 levels modulate meiotic spindle size and architecture in *Xenopus* egg extracts. *J. Cell Biol.* 206:385–393. http://dx.doi.org/10.1083/jcb.201401014

Hirota, T., N. Kunitoku, T. Sasayama, T. Marumoto, D. Zhang, M. Nitta, K. Hatakeyama, and H. Saya. 2003. Aurora-A and an interacting activator, the LIM protein Ajuba, are required for mitotic commitment in human cells. *Cell.* 114:585–598. http://dx.doi.org/10.1016/S0092-8674(03)00642-1

Kettenbach, A.N., D.K. Schweppe, B.K. Faherty, D. Pechenick, A.A. Pletnev, and S.A. Gerber. 2011. Quantitative phosphoproteomics identifies substrates and functional modules of Aurora and Polo-like kinase activities in mitotic cells. *Sci. Signal.* 4:rs5. http://dx.doi.org/10.1126/scisignal.2001497

Kufer, T.A., H.H. Silljé, R. Körner, O.J. Gruss, P. Meraldi, and E.A. Nigg. 2002. Human TPX2 is required for targeting Aurora-A kinase to the spindle. *J. Cell Biol.* 158:617–623. http://dx.doi.org/10.1083/jcb.200204155

Kwok, B.H., and T.M. Kapoor. 2007. Microtubule flux: drivers wanted. *Curr. Opin. Cell Biol.* 19:36–42. http://dx.doi.org/10.1016/j.ceb.2006.12.003

Laycock, J.E., M.S. Savoian, and D.M. Glover. 2006. Antagonistic activities of Klp10A and Orbit regulate spindle length, bipolarity and function in vivo. *J. Cell Sci.* 119:2354–2361. http://dx.doi.org/10.1242/jcs.02957

Liu, J., Z. Wang, K. Jiang, L. Zhang, L. Zhao, S. Hua, F. Yan, Y. Yang, D. Wang, C. Fu, et al. 2009. PRC1 cooperates with CLASP1 to organize central spindle plasticity in mitosis. *J. Biol. Chem.* 284:23059–23071. http://dx.doi.org/10.1074/jbc.M109.009670

Ma, N., U.S. Tulu, N.P. Ferenz, C. Fagerstrom, A. Wilde, and P. Wadsworth. 2010. Poleward transport of TPX2 in the mammalian mitotic spindle requires dynein, Eg5, and microtubule flux. *Mol. Biol. Cell.* 21:979–988. http://dx.doi.org/10.1091/mbc.E09-07-0601

Ma, N., J. Titus, A. Gable, J.L. Ross, and P. Wadsworth. 2011. TPX2 regulates the localization and activity of Eg5 in the mammalian mitotic spindle. *J. Cell Biol.* 195:87–98. http://dx.doi.org/10.1083/jcb.201106149

Maffini, S., A.R. Maia, A.L. Manning, Z. Maliga, A.L. Pereira, M. Junqueira, A. Shevchenko, A. Hyman, J.R. Yates III, N. Galjart, et al. 2009. Motor-independent targeting of CLASPs to kinetochores by CENP-E promotes microtubule turnover and poleward flux. *Curr. Biol.* 19:1566–1572. http://dx.doi.org/10.1016/j.cub.2009.07.059

Maiato, H., E.A. Fairley, C.L. Rieder, J.R. Swedlow, C.E. Sunkel, and W.C. Earnshaw. 2003. Human CLASP1 is an outer kinetochore component that regulates spindle microtubule dynamics. *Cell.* 113:891–904. http://dx.doi.org/10.1016/S0092-8674(03)00465-3

Maiato, H., A. Khodjakov, and C.L. Rieder. 2005. *Drosophila* CLASP is required for the incorporation of microtubule subunits into fluxing kinetochore fibres. *Nat. Cell Biol.* 7:42–47. http://dx.doi.org/10.1038/ncb1207

Mimori-Kiyosue, Y., I. Grigoriev, G. Lansbergen, H. Sasaki, C. Matsui, F. Severin, N. Galjart, F. Grosveld, I. Vorobjev, S. Tsukita, and A. Akhmanova. 2005. CLASP1 and CLASP2 bind to EB1 and regulate microtubule plus-end dynamics at the cell cortex. *J. Cell Biol.* 168:141–153. http://dx.doi.org/10.1083/jcb.200405094

Ohashi, S., G. Sakashita, R. Ban, M. Nagasawa, H. Matsuzaki, Y. Murata, H. Taniguchi, H. Shima, K. Furukawa, and T. Urano. 2006. Phosphoregulation of human protein kinase Aurora-A: analysis using anti-phospho-Thr288 monoclonal antibodies. *Oncogene.* 25:7691–7702. http://dx.doi.org/10.1038/sj.onc.1209754

Patel, K., E. Nogales, and R. Heald. 2012. Multiple domains of human CLASP contribute to microtubule dynamics and organization in vitro and in *Xenopus* egg extracts. *Cytoskeleton (Hoboken).* 69:155–165. http://dx.doi.org/10.1002/cm.21005

Petry, S., A.C. Groen, K. Ishihara, T.J. Mitchison, and R.D. Vale. 2013. Branching microtubule nucleation in *Xenopus* egg extracts mediated by augmin and TPX2. *Cell.* 152:768–777. http://dx.doi.org/10.1016/j.cell.2012.12.044

Reis, R., T. Feijão, S. Gouveia, A.J. Pereira, I. Matos, P. Sampaio, H. Maiato, and C.E. Sunkel. 2009. Dynein and mast/orbit/CLASP have antagonistic roles in regulating kinetochore-microtubule plus-end dynamics. *J. Cell Sci.* 122:2543–2553. http://dx.doi.org/10.1242/jcs.044818

Sardon, T., R.A. Pache, A. Stein, H. Molina, I. Vernos, and P. Aloy. 2010. Uncovering new substrates for Aurora A kinase. *EMBO Rep.* 11:977–984. http://dx.doi.org/10.1038/embor.2010.171

Schatz, C.A., R. Santarella, A. Hoenger, E. Karsenti, I.W. Mattaj, O.J. Gruss, and R.E. Carazo-Salas. 2003. Importin α-regulated nucleation of microtubules by TPX2. *EMBO J.* 22:2060–2070. http://dx.doi.org/10.1093/emboj/cdg195

Shrestha, R.L., N. Tamura, A. Fries, N. Levin, J. Clark, and V.M. Draviam. 2014. TAO1 kinase maintains chromosomal stability by facilitating proper congression of chromosomes. *Open Biol.* 4:130108. http://dx.doi.org/10.1098/rsob.130108

Torres, J.Z., J.J. Miller, and P.K. Jackson. 2009. High-throughput generation of tagged stable cell lines for proteomic analysis. *Proteomics.* 9:2888–2891. http://dx.doi.org/10.1002/pmic.200800873

Tsai, M.Y., C. Wiese, K. Cao, O. Martin, P. Donovan, J. Ruderman, C. Prigent, and Y. Zheng. 2003. A Ran signalling pathway mediated by the mitotic kinase Aurora A in spindle assembly. *Nat. Cell Biol.* 5:242–248. http://dx.doi.org/10.1038/ncb936

Wilbur, J.D., and R. Heald. 2013. Mitotic spindle scaling during *Xenopus* development by kif2a and importin α. *eLife.* 2:e00290. http://dx.doi.org/10.7554/eLife.00290